

$\sqrt{3}$ -Subdivision

Leif Kobbelt*

Max-Planck Institute for Computer Sciences

Abstract

A new stationary subdivision scheme is presented which performs *slower* topological refinement than the usual dyadic split operation. The number of triangles increases in every step by a factor of 3 instead of 4. Applying the subdivision operator *twice* causes a uniform refinement with *tri*-section of every original edge (hence the name $\sqrt{3}$ -subdivision) while two dyadic splits would *quad*-sect every original edge. Besides the finer gradation of the hierarchy levels, the new scheme has several important properties: The stencils for the subdivision rules have minimum size and maximum symmetry. The smoothness of the limit surface is C^2 everywhere except for the extraordinary points where it is C^1 . The convergence analysis of the scheme is presented based on a new general technique which also applies to the analysis of other subdivision schemes. The new splitting operation enables locally adaptive refinement under built-in preservation of the mesh consistency without temporary crack-fixing between neighboring faces from different refinement levels. The size of the surrounding mesh area which is affected by selective refinement is smaller than for the dyadic split operation. We further present a simple extension of the new subdivision scheme which makes it applicable to meshes with boundary and allows us to generate sharp feature lines.

1 Introduction

The use of subdivision schemes for the efficient generation of freeform surfaces has become commonplace in a variety of geometric modeling applications. Instead of defining a parametric surface by a functional expression $F(u, v)$ to be evaluated over a planar parameter domain $\Omega \in \mathbb{R}^2$ we simply sketch the surface by a coarse control mesh \mathcal{M}_0 that may have arbitrary connectivity and (manifold) topology. By applying a set of refinement rules, we generate a sequence of finer and finer meshes $\mathcal{M}_1, \dots, \mathcal{M}_k, \dots$ which eventually converge to a smooth limit surface \mathcal{M}_∞ .

In the literature there have been proposed many subdivision schemes which are either generalized from tensor-products of curve generation schemes [DS78, CC78, Kob96] or from 2-scale relations in more general functional spaces being defined over the three-directional grid [Loo87, DGL90, ZSS96]. Due to the nature of the refinement operators, the generalized tensor-product schemes natu-

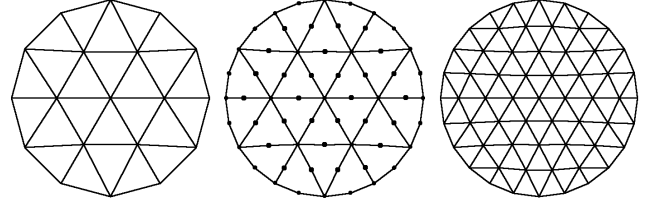


Figure 1: Subdivision schemes on triangle meshes are usually based on the 1-to-4 split operation which inserts a new vertex for every edge of the given mesh and then connects the new vertices.

rally lead to quadrilateral meshes while the others lead to triangle meshes.

A subdivision operator for polygonal meshes can be considered as being composed by a (topological) split operation followed by a (geometric) smoothing operation. The split operation performs the actual refinement by introducing new vertices and the smoothing operation changes the vertex positions by computing averages of neighboring vertices (generalized convolution operators, relaxation). In order to guarantee that the subdivision process will always generate a sequence of meshes \mathcal{M}_k that converges to a smooth limit, the smoothing operator has to satisfy specific necessary and sufficient conditions [CDM91, Dyn91, Rei95, Zor97, Pra98]. This is why special attention has been paid by many authors to the design of optimal smoothing rules and their analysis.

While in the context of quad-meshes several different topological split operations (e.g. primal [CC78, Kob96] or dual [DS78]) have been investigated, all currently proposed stationary schemes for triangle meshes are based on the uniform 1-to-4 split [Loo87, DGL90, ZSS96] which is depicted in Fig 1. This split operation introduces a new vertex for each edge of the given mesh.

Recently, the concept of uniform refinement has been generalized to *irregular* refinement [GSS99, KCVS98, VG99] where new vertices can be inserted at arbitrary locations without necessarily generating semi-uniform meshes with so-called *subdivision connectivity*. However, the convergence analysis of such schemes is still an open question.

In this paper we will present a new subdivision scheme for triangle meshes which is based on an alternative uniform split operator that introduces a new vertex for every *triangle* of the given mesh (Section 2).

As we will see in the following sections, the new split operator enables us to define a natural stationary subdivision scheme which has stencils of minimum size and maximum symmetry (Section 3). The smoothing rules of the subdivision operator are derived from well-known necessary conditions for the convergence to smooth limit surfaces. Since the standard subdivision analysis machinery cannot be applied directly to the new scheme, we derive a modified technique and prove that the scheme generates C^2 surfaces for regular control meshes. For arbitrary control meshes we find the limit surface to be C^2 almost everywhere except for the extraordinary vertices (valence $\neq 6$) where the smoothness is at least C^1 (see the Appendix).

*Max-Planck Institute for Computer Sciences, Im Stadtwald, 66123 Saarbrücken, Germany, kobbelt@mpi-sb.mpg.de

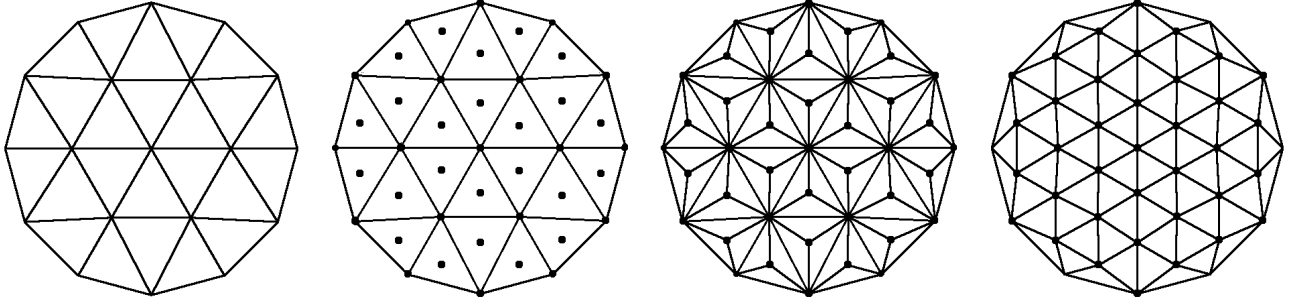


Figure 2: The $\sqrt{3}$ -subdivision scheme is based on a split operation which first inserts a new vertex for every face of the given mesh. Flipping the original edges then yields the final result which is a 30 degree rotated regular mesh. Applying the $\sqrt{3}$ -subdivision scheme twice leads to a 1-to-9 refinement of the original mesh. As this corresponds to a tri-adic split (two new vertices are introduced for every original edge) we call our scheme $\sqrt{3}$ -subdivision.

Inserting a new vertex into a triangular face does only affect that single face which makes locally adaptive refinement very effective. The global consistency of the mesh is preserved automatically if $\sqrt{3}$ -subdivision is performed selectively. In Section 4 we compare adaptively refined meshes generated by dyadic subdivision with our $\sqrt{3}$ -subdivision meshes and find that $\sqrt{3}$ -subdivision usually needs fewer triangles and less effort to achieve the same approximation tolerance. The reason for this effect is the better *localization*, i.e., only a relatively small region of the mesh is affected if more vertices are inserted locally.

For the generation of surfaces with smooth boundary curves, we need special smoothing rules at the boundary faces of the given mesh. In Section 5 we propose a boundary rule which reproduces cubic B-splines. The boundary rules can also be used to generate sharp feature lines in the interior of the surface.

2 $\sqrt{3}$ -Subdivision

The most wide-spread way to uniformly refine a given triangle mesh \mathcal{M}_0 is the *dyadic split* which bi-sects all the edges by inserting a new vertex between every adjacent pair of old ones. Each triangular face is then split into four smaller triangles by mutually connecting the new vertices sitting on a face's edges (cf. Fig. 1). This type of splitting has the positive effect that all newly inserted vertices have valence six and the valences of the old vertices does not change. After applying the dyadic split several times, the refined meshes \mathcal{M}_k have a semi-regular structure since the repeated 1-to-4 refinement replaces every triangle of the original mesh by a regular patch with 4^k triangles.

A straightforward generalization of the dyadic split is the n -adic split where every edge is subdivided into n segments and consequently every original face is split into n^2 sub-triangles. However, in the context of stationary subdivision schemes, the n -adic split operation requires a specific smoothing rule for every new vertex (modulo permutations of the barycentric coordinates). This is why subdivision schemes are mostly based on the dyadic split that only requires two smoothing rules: one for the old vertices and one for the new ones (plus rotations).

In this paper, we consider the following refinement operation for triangle meshes: Given a mesh \mathcal{M}_0 we perform a 1-to-3 split for every triangle by inserting a new vertex at its center. This introduces three new edges connecting the new vertex to the surrounding old ones. In order to re-balance the valence of the mesh vertices we then flip every original edge that connects two old vertices (cf. Fig. 2).

This split operation is uniform in the sense that if it is applied to a uniform (three-directional) grid, a (rotated and refined) uniform grid is generated (cf. Fig. 2). If we apply the same refinement operator twice, the combined operator splits every original triangle into

nine subtriangles (*tri-adic split*). Hence one single refinement step can be considered as the "square root" of the tri-adic split. In a different context, this type of refinement operator has been considered independently in [Sab87] and [Gus98].

Analyzing the action of the $\sqrt{3}$ -subdivision operator on arbitrary triangle meshes, we find that all newly inserted vertices have exactly valence six. The valences of the old vertices are not changed such that after a sufficient number of refinement steps, the mesh \mathcal{M}_k has large regions with regular mesh structure which are disturbed only by a small number of isolated extraordinary vertices. These correspond to the vertices in \mathcal{M}_0 which had valence $\neq 6$ (cf. Fig. 3).

There are several arguments why it is interesting to investigate this particular refinement operator. First, it is very *natural* to subdivide triangular faces at their center rather than splitting all three edges since the coefficients of the subsequent smoothing operator can reflect the threefold symmetry of the three-directional grid.

Second, the $\sqrt{3}$ -refinement is in some sense *slower* than the standard refinement since the number of vertices (and faces) increases by the factor of 3 instead of 4. As a consequence, we have more levels of uniform resolution if a prescribed target complexity of the mesh must not be exceeded. This is why similar uniform refinement operators for quad-meshes have been used in numerical applications such as multi-grid solvers for finite element analysis [Hac85, GZZ93].

From the computer graphics point of view the $\sqrt{3}$ -refinement has the nice property that it enables a very simple implementation of adaptive refinement strategies with no inconsistent intermediate states as we will see in Section 4.

In the context of polygonal mesh based multiresolution representations [ZSS96, KCVS98, GSS99], the $\sqrt{3}$ -hierarchies can provide an intuitive and robust way to encode the detail information since the detail coefficients are assigned to faces (\approx tangent planes) instead of vertices.

3 Stationary smoothing rules

To complete the definition of our new subdivision scheme, we have to find the two smoothing rules, one for the placement of the newly inserted vertices and one for the relaxation of the old ones. For the sake of efficiency, our goal is to use the smallest possible stencils while still generating high quality meshes.

There are well-known necessary and sufficient criteria which tell whether a subdivision scheme S is convergent or not and what smoothness properties the limit surface has. Such criteria check if the eigenvalues of the *subdivision matrix* have a certain distribution and if a local regular parameterization exists in the vicinity of every vertex on the limit surface [CDM91, Dyn91, Rei95, Zor97, Pra98].

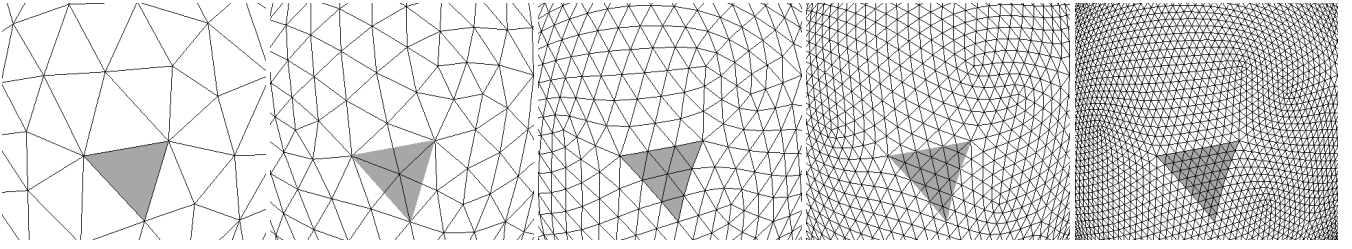


Figure 3: The $\sqrt{3}$ -subdivision generates semi-regular meshes since all new vertices have valence six. After an even number $2k$ of refinement steps, each original triangle is replaced by a regular patch with 9^k triangles.

By definition, the subdivision matrix is a square matrix S which maps a certain sub-mesh $\mathbf{V} \in \mathcal{M}_k$ to a topologically equivalent sub-mesh $S(\mathbf{V}) \in \mathcal{M}_{k+1}$ of the refined mesh. Every row of this matrix is a rule to compute the position of a new vertex. Every column of this matrix tells how one old vertex contributes to the vertex positions in the refined mesh. Usually, \mathbf{V} is chosen to be the neighborhood of a particular vertex, e.g., a vertex \mathbf{p} and its neighbors up to the k -th order (k -ring neighborhood).

To derive the weight coefficients for the new subdivision scheme, we use these criteria for some kind of *reverse engineering* process, i.e., instead of analyzing a given scheme, we derive one which by construction satisfies the known necessary criteria. The justification for doing this is that if the necessary conditions uniquely determine a smoothing rule then the resulting subdivision scheme is the *only* scheme (with the given stencil) that is worth being considered. In the Appendix we will give the details of the sufficient part of the convergence analysis.

Since the $\sqrt{3}$ -subdivision operator inserts a new vertex for every triangle of the given mesh, the minimum stencil for the corresponding smoothing rule has to include at least the three (old) corner vertices of that triangle. For symmetry reasons, the only reasonable choice for that smoothing rule is hence

$$\mathbf{q} := \frac{1}{3} (\mathbf{p}_i + \mathbf{p}_j + \mathbf{p}_k), \quad (1)$$

i.e., the new vertex \mathbf{q} is simply inserted at the center of the triangle $\triangle(\mathbf{p}_i, \mathbf{p}_j, \mathbf{p}_k)$.

The smallest non-trivial stencil for the relaxation of the old vertices is the 1-ring neighborhood containing the vertex itself and its direct neighbors. To establish symmetry, we assign the same weight to each neighbor. Let \mathbf{p} be a vertex with valence n and $\mathbf{p}_0, \dots, \mathbf{p}_{n-1}$ its directly adjacent neighbors in the unrefined mesh then we define

$$S(\mathbf{p}) := (1 - \alpha_n) \mathbf{p} + \alpha_n \frac{1}{n} \sum_{i=0}^{n-1} \mathbf{p}_i. \quad (2)$$

The remaining question is what the optimal choice for the parameter α_n would be. Usually, the coefficient depends on the valence of \mathbf{p} in order to make the subdivision scheme applicable to control meshes \mathcal{M}_0 with arbitrary connectivity.

The rules (1) and (2) imply that the 1-ring neighborhood of a vertex $S(\mathbf{p}) \in \mathcal{M}_{k+1}$ only depends on the 1-ring neighborhood of the corresponding vertex $\mathbf{p} \in \mathcal{M}_k$. Hence, we can set-up a $(n+1) \times (n+1)$ matrix which maps \mathbf{p} and its n neighbors to the next refinement level. Arranging all the vertices in a vector

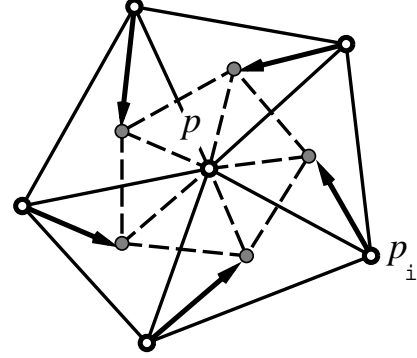


Figure 4: The application of the subdivision matrix S causes a rotation around \mathbf{p} since the neighboring vertices are replaced by the centers of the adjacent triangles.

$[\mathbf{p}, \mathbf{p}_0, \dots, \mathbf{p}_{n-1}]$ we derive the subdivision matrix

$$S = \frac{1}{3} \begin{pmatrix} u & v & v & v & \cdots & v \\ 1 & 1 & 1 & 0 & \cdots & 0 \\ 1 & 0 & \ddots & \ddots & \ddots & \vdots \\ \vdots & \vdots & \ddots & \ddots & \ddots & 0 \\ 1 & 0 & \ddots & \ddots & \ddots & 1 \\ 1 & 1 & 0 & \cdots & 0 & 1 \end{pmatrix} \quad (3)$$

with $u = 3(1 - \alpha_n)$ and $v = 3\alpha_n/n$. However, when analysing the eigenstructure of this matrix, we find that it is not suitable for the construction of a convergent subdivision scheme. The reason for this defect is the rotation around \mathbf{p} which is caused by the application of S and which makes all eigenvalues of S complex. Fig. 4 depicts the situation.

From the last section we know that applying the $\sqrt{3}$ -subdivision operator two times corresponds to a tri-adic split. So instead of analysing one single subdivision step, we can combine two successive steps since after the second application of S , the neighborhood of $S^2(\mathbf{p})$ is again aligned to the original configuration around \mathbf{p} . Hence, the back-rotation can be written as a simple permutation matrix

$$R = \begin{pmatrix} 1 & 0 & \cdots & 0 & 0 \\ 0 & 0 & \cdots & 0 & 1 \\ 0 & 1 & \ddots & & 0 \\ \vdots & \ddots & \ddots & \ddots & \vdots \\ 0 & \cdots & 0 & 1 & 0 \end{pmatrix}.$$

The resulting matrix $\tilde{S} = RS^2$ now has the correct eigenstructure for

the analysis. Its eigenvalues are:

$$\frac{1}{9} \left[9, (2 - 3\alpha_n)^2, 2 + 2 \cos(2\pi \frac{1}{n}), \dots, 2 + 2 \cos(2\pi \frac{n-1}{n}) \right] \quad (4)$$

From [Rei95, Zor97] it is known that for the leading eigenvalues, sorted by decreasing modulus, the following necessary conditions have to hold

$$\lambda_1 = 1 > \lambda_2 = \lambda_3 > \lambda_i, \quad i = 4, \dots, n+1. \quad (5)$$

Additionally, according to [Pra98, Zor97], a natural choice for the eigenvalue λ_4 is $\lambda_4 = \lambda_2^2$ since the eigenstructure of the subdivision matrix can be interpreted as a generalized Taylor-expansion of the limit surface at the point \mathbf{p} . The eigenvalue λ_4 then corresponds to a quadratic term in that expansion. Consequently, we define the value for α_n by solving

$$\left(\frac{2}{3} - \alpha_n \right)^2 = \left(\frac{2 + 2 \cos(2\pi \frac{1}{n})}{9} \right)^2$$

which leads to

$$\alpha_n = \frac{4 - 2 \cos(\frac{2\pi}{n})}{9} \quad (6)$$

where we picked that solution of the quadratic equation for which the coefficient α_n always stays in the interval $[0, 1]$ and (2) is a convex combination. The explanation for the existence of a second solution is that we actually analyse a double step $\tilde{S} = RS^2$. The real eigenvalue $(\frac{2}{3} - \alpha_n)^2$ of \tilde{S} corresponds to the eigenvalue $\frac{2}{3} - \alpha_n$ of S both with the same eigenvector $[-3\alpha_n, 1, \dots, 1]$ which is invariant under R . Obviously we have to choose α_n such that negative real eigenvalues of S are avoided [Rei95].

Equations (1), (2) and (6) together completely define the smoothing operator for our stationary subdivision scheme since they provide all the necessary information to implement the scheme. Notice that the spectral properties of the matrices S and \tilde{S} are not sufficient for the actual convergence analysis of the subdivision scheme. It is only used here to derive the smoothing rule from the necessary conditions! The sufficient part of the convergence analysis is presented in the Appendix.

4 Adaptive refinement strategies

Although the complexity of the refined meshes \mathcal{M}_k grows slower under $\sqrt{3}$ -subdivision than under dyadic subdivision (cf. Fig. 13), the number of triangles still increases exponentially. Hence, only relatively few refinement steps can be performed if the resulting meshes are to be processed on a standard PC. The common techniques to curb the mesh complexity under refinement are based on adaptive refinement strategies which insert new vertices only in those regions of the surface where more geometric detail is expected. Flat regions of the surface are sufficiently well approximated by large triangles.

The major difficulties that emerge from adaptive refinement are caused by the fact that triangles from different refinement levels have to be joined in a consistent manner (*conforming meshes*) which often requires additional redundancy in the underlying mesh data structure. To reduce the number of topological special cases and to guarantee a minimum quality of the resulting triangular faces, the adaptive refinement is usually restricted to *balanced meshes* where the refinement level of adjacent triangles must not differ by more than one generation. However, to maintain the mesh balance at any time, a local refinement step can trigger several additional split operations in its vicinity. This is the reason why adaptive refinement techniques are rated by their *localization* property, i.e.,

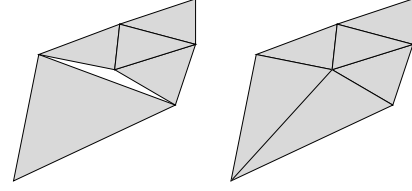


Figure 5: The gap between triangles from different refinement levels can be fixed by temporarily replacing the larger face by a triangle fan.

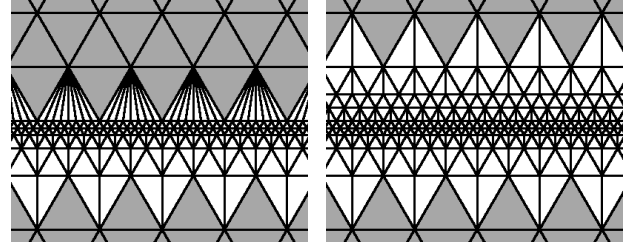


Figure 6: The gap fixing by triangle fans tends to produce degenerate triangles if the refinement is not balanced (left). Balancing the refinement, however, causes a larger region of the mesh to be affected by local refinement (right).

by the extend to which the side-effects of a local refinement step spread over the mesh.

For refinement schemes based on the dyadic split operation, the local splitting of one triangular face causes gaps if neighboring faces are not refined (cf. Fig. 5). These gaps have to be removed by replacing the adjacent (unrefined) faces with a triangle fan. As shown in Fig. 6 this simple strategy tends to generate very badly shaped triangles if no balance of the refinement is enforced.

If further split operations are applied to an already adaptively refined mesh, the triangle fans have to be removed first since the corresponding triangles are not part of the actual refinement hierarchy. The combination of dyadic refinement, mesh balancing and gap fixing by temporary triangle fans is well-known under the name *red-green triangulation* in the finite element community [VT92, Ver96].

There are several reason why $\sqrt{3}$ -subdivision seems better suited for adaptive refinement. First, the slower refinement reduces the expected average over-tessellation which occurs when a coarse triangle slightly fails the stopping criterion for the adaptive refinement but the result of the refinement falls significantly below the threshold.

The second reason is that the localization is better than for dyadic refinement and no temporary triangle fans are necessary to keep the mesh consistent. In fact, the consistency preserving adaptive refinement can be implemented by a simple recursive procedure. No refinement history has to be stored in the underlying data structure since no temporary triangles are generated which do not belong to the actual refinement hierarchy.

To implement the adaptive refinement, we have to assign a generation index to each triangle in the mesh. Initially all triangles of the given mesh \mathcal{M}_0 are generation 0. If a triangle with *even* generation index is split into three by inserting a new vertex at its center, the generation index increases by 1 (giving an odd index to the new triangles). Splitting a triangle with *odd* generation index requires to find its "mate", perform an edge flip, and assign even indices to the resulting triangles.

For an already adaptively refined mesh, further splits are performed by the following recursive procedure

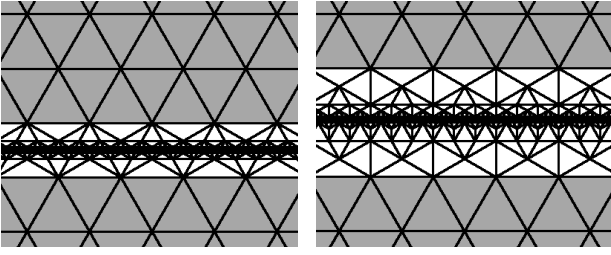


Figure 7: Adaptive refinement based on $\sqrt{3}$ -subdivision achieves an improved localization while automatically preventing degenerate triangles since all occurring triangles are a subset of the underlying hierarchy of uniformly refined meshes. Let us assume the horizontal coarse scale grid lines in the images have constant integer y coordinates then the two images result from adaptively refining all triangles that intersect a certain $y = \text{const.}$ line. In the left image y was chosen from $[\frac{1}{3}, \frac{2}{3}]$ and in the right image $y = 1 + \epsilon$ which explains the different localization.

```

split(T)
  if (T.index is even) then
    compute midpoint P
    split T(A,B,C) into T[1](P,A,B), T[2](P,B,C), T[3](P,C,A)
    for i = 1,2,3 do
      T[i].index = T.index + 1
      if (T[i].mate[1].index == T[i].index) then
        swap(T[i], T[i].mate[1])
      else
        if (T.mate[1].index == T.index - 2)
          split(T.mate[1])
        split(T.mate[1]) /* ... triggers edge swap */

```

which automatically preserves the mesh consistency and implicitly maintains some mild balancing condition for the refinement levels of adjacent triangles. Notice that the ordering of the vertices in the 1-to-3 split is chosen such that reference `mate[1]` always points to the correct neighboring triangle (outside the parent triangle T). The edge flipping procedure is implemented as

```

swap(T1, T2)

change T1(A,B,C), T2(B,A,D) into T1(C,A,D), T2(D,B,C)
T1.index++
T2.index++

```

All the triangles that are generated during the adaptive $\sqrt{3}$ -refinement form a proper subset of the uniform refinement hierarchy. This implies that the shape of the triangles does never degenerate. The worst triangles are those generated by an 1-to-3 split. Edge flipping then mostly re-improves the shape. Fig. 7 shows two adaptively refined example meshes. Another approach to adaptive mesh refinement with built-in consistency is suggested in [VG00].

When adaptive refinement is performed in the context of stationary subdivision, another difficulty arises from the fact that for the application of the smoothing rules a certain neighborhood of vertices from the same refinement level has to be present. This puts some additional constraints on the mesh balance. In [ZSS97] this is explained for Loop subdivision with dyadic refinement.

For $\sqrt{3}$ -subdivision it is sufficient to slightly modify the recursive splitting procedure such that *before* splitting an even-indexed triangle by vertex insertion, all older odd-indexed neighbors have to be split (even-indexed neighbors remain untouched). This guarantees that enough information is available for later applications of the smoothing rule (2). The rule (1) is always applicable since it only uses the three vertices of the current triangle. Notice that the

1-to-3 split is the only way new vertices enter the mesh. Moreover, every new vertex eventually has valence six — although some of its neighbors might not yet be present.

The modification of the recursive procedure implies that when a new vertex \mathbf{p} is inserted, its neighboring vertices $\mathbf{p}_1, \dots, \mathbf{p}_6$ either exist already, or at least the triangles exist at whose centers these vertices are going to be inserted. In any case it is straightforward to compute the average $\frac{1}{n} \sum_i \mathbf{p}_i$ which is all we need for the application of (2).

The remaining technical problem is that in an adaptively refined mesh, the geometric location of a mesh vertex is not always well-defined. Ambiguities occur if triangles from different refinement levels share a common vertex since the smoothing rule (2) is non-interpolatory. We solved this problem by implementing a multi-step smoothing rule which enables direct access to the vertex positions at any refinement level. Accessing a `Vertex-object` by `Vertex::pos(k)` returns the vertex coordinates corresponding to the k th refinement level. `Vertex::pos(inf)` returns the corresponding point on the limit surface which is the location that is eventually used for display.

Multi-step rules are generalizations of the rule (2) which allow direct evaluation of arbitrary powers of S . As we already discussed in Section 3, the 1-ring neighborhood $[\mathbf{p}, \mathbf{p}_0, \dots, \mathbf{p}_{n-1}]$ of a vertex \mathbf{p} is mapped to (a scaled version of) itself under application of the subdivision scheme. This is reflected by the matrix S in (3). If we compute the m th power of the subdivision matrix in (3), we find in the first row a linear combination of $[\mathbf{p}, \mathbf{p}_0, \dots, \mathbf{p}_{n-1}]$ which directly yields $S^m(\mathbf{p})$. For symmetry reason this multi-step rule can, again, be written as a linear combination of the original vertex \mathbf{p} and the average of its neighbors $\frac{1}{n} \sum_i \mathbf{p}_i$.

By eigenanalysis of the matrix S it is fairly straightforward to derive a closed form solution for the multi-step rule [Sta98]:

$$S^m(\mathbf{p}) := (1 - \beta_n(m)) \mathbf{p} + \beta_n(m) \frac{1}{n} \sum_{i=0}^{n-1} \mathbf{p}_i \quad (7)$$

with

$$\beta_n(m) = \frac{3\alpha_n - 3\alpha_n(\frac{2}{3} - \alpha_n)^m}{1 + 3\alpha_n}$$

especially

$$\beta_n(\infty) = \frac{3\alpha_n}{1 + 3\alpha_n}.$$

Since the point $\mathbf{p}^{(\infty)} = S^\infty(\mathbf{p})$ on the limit surface is particularly important, we rewrite (7) by eliminating the average of \mathbf{p} 's neighbors

$$S^m(\mathbf{p}) := \gamma_n(m) \mathbf{p} + (1 - \gamma_n(m)) \mathbf{p}^{(\infty)} \quad (8)$$

with

$$\gamma_n(m) = \left(\frac{2}{3} - \alpha_n\right)^m.$$

In our implementation, every `Vertex-object` stores its original position \mathbf{p} (at the time it was inserted into the mesh) and its limit position $\mathbf{p}^{(\infty)}$. The vertex position at arbitrary levels can then be computed by (8).

5 Boundaries

In practical and industrial applications it is usually necessary to be able to process control meshes with well-defined boundary polygons which should result in surfaces with smooth boundary curves. As the neighborhood of boundary vertices is not complete, we have to figure out special refinement and smoothing rules.

When topologically refining a given open control mesh \mathcal{M}_0 by the $\sqrt{3}$ -operator we split all triangular faces 1-to-3 but flip only the

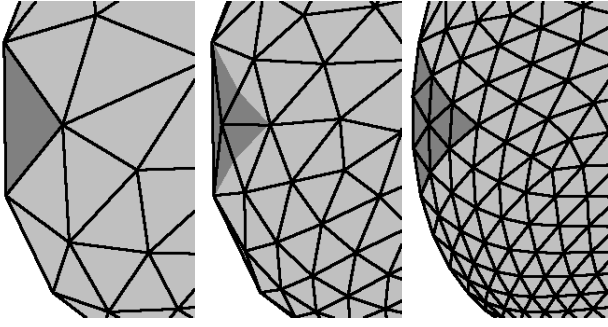


Figure 8: The boundary is subdivided only in every other step such that a uniform 1-to-9 refinement of the triangular faces is achieved.

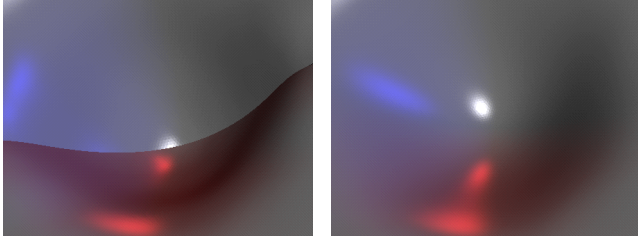


Figure 9: The use of univariate smoothing rules at the boundaries enables the generation of sharp feature lines where two separate control meshes share an identical boundary polygon.

interior edges. Edge flipping at the boundaries is not possible since the opposite triangle-mate is missing. Hence, the boundary polygon is not modified in the first $\sqrt{3}$ -subdivision step.

As we already discussed in Section 2, the application of a second $\sqrt{3}$ -step has the overall effect of a tri-adic split where each original triangle is replaced by 9 new ones. Consequently, we have to apply a univariate tri-section rule to the boundary polygon and connect the new vertices to the corresponding interior ones such that a uniform 1-to-9 split is established for each boundary triangle (cf. Fig. 8).

The smoothing rules at the boundaries should only use boundary vertices and no interior ones. This is the simplest way to enable the generation of C^0 creases in the interior of the surface (*feature lines*) since it guarantees that control meshes with identical boundary polygons will result in smooth surfaces with identical boundary curves [HDD+94] (cf. Fig. 9). More sophisticated techniques for the design of optimal boundary smoothing rules with normal control can be found in [BLZ99].

For our $\sqrt{3}$ -subdivision scheme we choose, for simplicity, a univariate boundary subdivision scheme which reproduces cubic splines (maximum smoothness, minimum stencil). From the trivial tri-section mask for linear splines we can easily obtain the corresponding tri-section mask for cubic splines by convolution

$$\begin{aligned} & \frac{1}{3} [1, 2, 3, 2, 1] * \left(\frac{1}{3} [1, 1, 1] \right)^2 \\ &= \frac{1}{9} [1, 3, 6, 7, 6, 3, 1] * \frac{1}{3} [1, 1, 1] \\ &= \frac{1}{27} [1, 4, 10, 16, 19, 16, 10, 4, 1] \end{aligned}$$

Hence the resulting smoothing rules are

$$\begin{aligned} \mathbf{p}'_{3i-1} &= \frac{1}{27} (10\mathbf{p}_{i-1} + 16\mathbf{p}_i + \mathbf{p}_{i+1}) \\ \mathbf{p}'_{3i} &= \frac{1}{27} (4\mathbf{p}_{i-1} + 19\mathbf{p}_i + 4\mathbf{p}_{i+1}) \\ \mathbf{p}'_{3i+1} &= \frac{1}{27} (\mathbf{p}_{i-1} + 16\mathbf{p}_i + 10\mathbf{p}_{i+1}). \end{aligned} \quad (9)$$

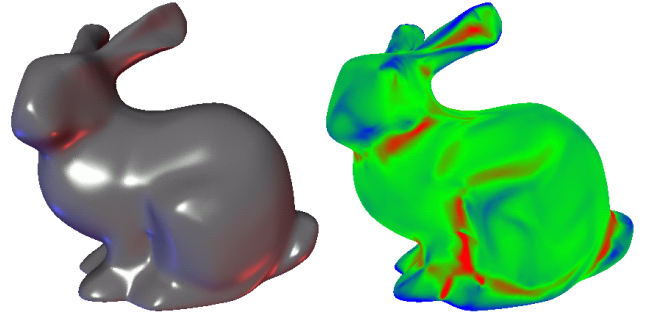


Figure 10: A decimated Stanford bunny was used as a subdivision control mesh \mathcal{M}_0 . We applied the $\sqrt{3}$ -subdivision scheme 4 times (left). The right image shows the mean curvature distribution.

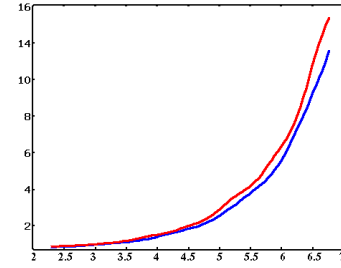


Figure 11: This plot shows the triangle count (Y : in $K\Delta$) vs. approximation error (X : in $-\log(\epsilon)$). The red curve is the complexity of the Loop-meshes, the blue curve the complexity of the $\sqrt{3}$ -meshes. The ratio lies between 5% and 25%.

6 Examples

To demonstrate the quality of the $\sqrt{3}$ -subdivision surfaces we show a mesh generated by uniformly refining a decimated version of the Stanford bunny (cf. Fig 10). The C^2 smoothness of the limit surface guarantees curvature continuity and the relaxing properties of the smoothing rules with only positive weights lead to a fair distribution of the curvature.

We made several numerical experiments to check the relative complexity of the adaptively refined meshes \mathcal{M}_k generated either by $\sqrt{3}$ -subdivision or by Loop-subdivision. For the stopping criterion in the adaptive refinement we used the local approximation error of the current mesh (with all vertices projected onto the limit surface) to the limit surface. A reliable estimation of the exact approximation error can be computed by constructing tight bounding envelopes as described in [KDS98].

After testing various models with different geometric complexities over the range $[10^{-2}, 10^{-7}]$ for the approximation tolerance, we found that adaptive $\sqrt{3}$ -subdivision meshes usually need fewer triangles than adaptive Loop-subdivision surfaces to obtain the same approximation tolerance. The improvement is typically between 5% and 25% with an average at 10%. Fig. 11 shows the typical relation between approximation tolerance and mesh complexity.

Fig. 12 shows another example mesh generated by the adaptive $\sqrt{3}$ -subdivision scheme in comparison to the corresponding Loop subdivision surface defined by the same control mesh. This time we use a *curvature* dependent adaptive refinement strategy: The subdivision level is determined by a discrete local curvature estimation.

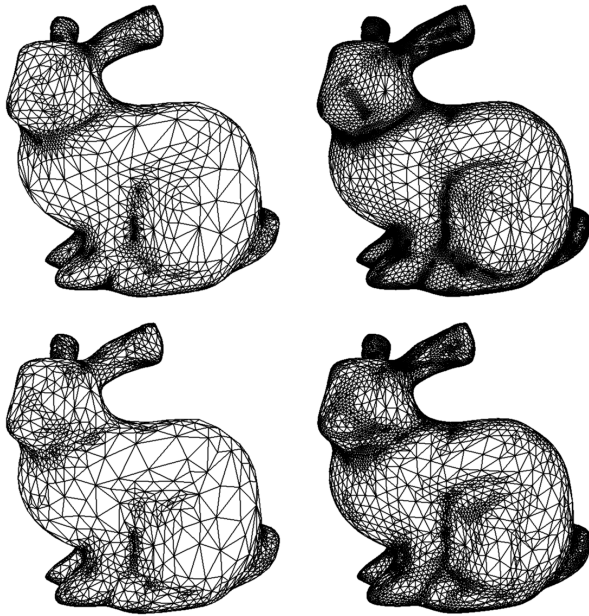


Figure 12: Adaptive refinement based on red-green triangulation with Loop subdivision (top row) and based on the $\sqrt{3}$ -refinement (bottom row). While the same stopping criterion is used (left and right respectively), the Loop meshes have 10072 and 28654 triangles while the $\sqrt{3}$ -meshes only have 7174 and 20772 triangles.

7 Conclusion

We presented a new stationary subdivision scheme which iteratively generates high quality C^2 surfaces with minimum computational effort. It shares the advantages of the well-known standard schemes but has important additional properties. Especially the slower increase of the mesh complexity and the suitability for adaptive refinement with automatic consistency preservation makes it a promising approach for practical and industrial applications.

The analysis technique we present in the Appendix provides a simple tool to analyse a very general class of subdivision schemes which are not necessarily based on some known polynomial spline basis function and not generated by taking the tensor-product of some univariate scheme.

Future modifications and extensions of the $\sqrt{3}$ -subdivision scheme should aim at incorporating more sophisticated boundary rules [BLZ99] and interpolation constraints [Lev99]. Modifications of the smoothing rules with different stencils could lead to new subdivision schemes with interesting properties.

Acknowledgements

I would like to thank Stephan Bischoff and Ulf Labsik for implementing the $\sqrt{3}$ -subdivision scheme and performing some of the experiments.

References

[BLZ99] H. Biermann, A. Levin, D. Zorin, *Piecewise smooth subdivision surfaces with normal control*, Preprint

[CC78] E. Catmull, J. Clark, *Recursively generated B-spline surfaces on arbitrary topological meshes*, CAD **10** (1978), 350–355

[CDM91] A. Cavaretta, W. Dahmen, C. Micchelli, *Stationary Subdivision*, Memoirs of the AMS **93** (1991), pp. 1–186

[DS78] D. Doo, M. Sabin, *Behaviour of recursive division surfaces near extraordinary points*, CAD **10** (1978), 356–360

[DGL90] N. Dyn, J. Gregory, D. Levin, *A Butterfly Subdivision Scheme for Surface Interpolation with Tension Control*, ACM Trans. Graph. **9** (1990), pp. 160–169

[Dyn91] N. Dyn, *Subdivision Schemes in Computer Aided Geometric Design*, Advances in Numerical Analysis II, Wavelets, Subdivisions and Radial Functions, W.A. Light ed., Oxford University Press, 1991, pp. 36–104.

[GSS99] I. Guskov, W. Sweldens, P. Schröder, *Multiresolution signal processing for meshes*, SIGGRAPH 99 Proceedings, 1999, pp. 325 – 334

[GvL96] G. Golub, C. van Loan, *Matrix Computations*, 3rd, Johns Hopkins Univ Press, 1996

[GZZ93] M. Griebel, C. Zenger, S. Zimmer, *Multilevel Gauss-Seidel-Algorithms for Full and Sparse Grid Problems*, Computing **50**, 1993, pp. 127–148

[Gus98] I. Guskov, *Multivariate subdivision schemes and divided differences*, Preprint, Princeton University, 1998

[Hac85] W. Hackbusch, *Multi-Grid Methods and Applications*, Springer, Berlin, 1985

[HDD+94] H. Hoppe, T. DeRose, T. Duchamp, M. Halstead, H. Jin, J. McDonald, J. Schweitzer, W. Stuetzle, *Piecewise smooth surface reconstruction*, SIGGRAPH 1994 Proceedings, 1994, pp. 295–302

[Kob96] L. Kobbelt, *Interpolatory Subdivision on Open Quadrilateral Nets with Arbitrary Topology*, Computer Graphics Forum **15** (1996), Eurographics '96 Conference Issue, pp. 409–420

[KDS98] L. Kobbelt, K. Daubert, H-P. Seidel, *Ray-tracing of subdivision surfaces*, 9th Eurographics Workshop on Rendering Proceedings, 1998, pp. 69 – 80

[KCVS98] L. Kobbelt, S. Campagna, J. Vorsatz, H-P. Seidel, *Interactive multiresolution modeling on arbitrary meshes*, SIGGRAPH 98 Proceedings, 1998, pp. 105–114

[Lev99] A. Levin, *Interpolating nets of curves by smooth subdivision surfaces*, SIGGRAPH 99 Proceedings, 1999, pp. 57 – 64

[Loo87] C. Loop, *Smooth subdivision surfaces based on triangles*, Master Thesis, Utah University, USA, 1987

[Pra98] H. Prautzsch, *Smoothness of subdivision surfaces at extraordinary points*, Adv. Comp. Math. **14** (1998), pp. 377 – 390

[Rei95] U. Reif, *A unified approach to subdivision algorithms near extraordinary vertices*, CAGD **12** (1995), pp. 153–174

[RP98] U. Reif, J. Peters, *The simplest subdivision scheme for smoothing polyhedra*, ACM Trans. Graph. **16** (1998), pp. 420 – 431

[Sab87] M. Sabin, *Recursive Division*, in The Mathematics of Surfaces, Clarendon Press, 1986, pp. 269 – 282

[Sta98] J. Stam, *Exact evaluation of Catmull/Clark subdivision surfaces at arbitrary parameter values*, SIGGRAPH 98 Proceeding, 1998, pp. 395 – 404

[VG99] L. Velho, J. Gomes, *Quasi-stationary subdivision using four directional meshes*, Preprint

[VG00] L. Velho, J. Gomes, *Semi-regular 4-8 refinement and box spline surfaces*, Preprint

[VT92] M. Vasilescu, D. Terzopoulos, *Adaptive meshes and shells: Irregular triangulation, discontinuities and hierarchical subdivision*, Proceedings of the Computer Vision and Pattern Recognition Conference, 1992, 829 – 832

[Ver96] R. Verfürth, *A review of a posteriori error estimation and adaptive mesh refinement techniques*, Wiley-Teubner, 1996

[War00] J. Warren, *Subdivision methods for geometric design*, unpublished manuscript

[ZSS96] D. Zorin, P. Schröder, W. Sweldens, *Interpolating Subdivision for Meshes with Arbitrary Topology*, SIGGRAPH 96 Proceedings, 1996, pp. 189–192

[Zor97] D. Zorin, *C^k Continuity of Subdivision Surfaces*, Thesis, California Institute of Technology, 1997

[ZSS97] D. Zorin, P. Schröder, W. Sweldens, *Interactive multiresolution mesh editing*, SIGGRAPH 97 Proceedings, 1997, pp. 259–268

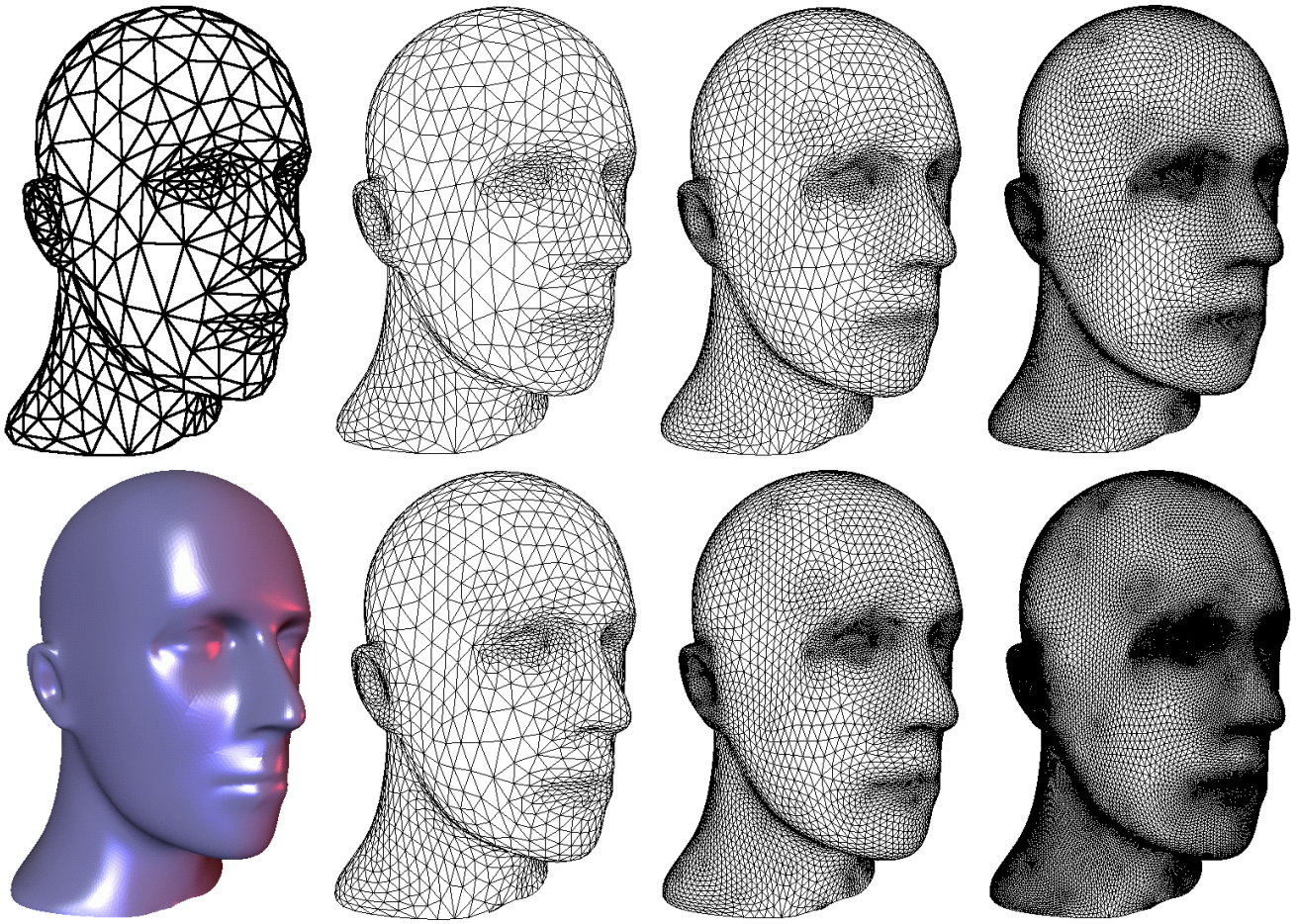


Figure 13: Sequences of meshes generated by the $\sqrt{3}$ -subdivision scheme (top row) and by the Loop subdivision scheme (bottom row). Although the quality of the limit surfaces is the same (C^2), $\sqrt{3}$ -subdivision uses an alternative refinement operator that increases the number of triangles slower than Loop's. The relative complexity of the corresponding meshes from both rows is (from left to right) $\frac{3}{4} = 0.75$, $\frac{9}{16} = 0.56$, and $\frac{27}{64} = 0.42$. Hence the new subdivision scheme yields a much finer gradation of uniform hierarchy levels.

Appendix: Convergence analysis

The convergence analysis of stationary subdivision schemes is generally done in two steps. In the first step, the smoothness of the limit surface is shown for *regular* meshes, i.e. for triangle meshes with all vertices having valence 6. Due to the nature of the topological refinement operator, subdivided meshes \mathcal{M}_k are regular almost everywhere. Once the regular case is shown, the convergence in the vicinity of extraordinary vertices (with valence $\neq 6$) can be proven. For many existing subdivision schemes, the first part of the proof is trivial since a closed form representation of the limit surface in the regular case is known, e.g. B-splines for Catmull/Clark or Doo/Sabin surfaces, Box-splines for Loop-surfaces.

For the two steps in the proof different techniques have to be used. The smoothness of the limit surface for regular control meshes follows from the *contractivity* of certain difference schemes S_n . These are generalized subdivision schemes which map directional forward differences of control points directly to directional forward differences (instead of the original subdivision scheme S mapping control points to control points).

In the vicinity of the extraordinary vertices, the convergence analysis is based on the eigenstructure of the local subdivision matrix. It is important to notice that the criteria for the eigenstructure of the subdivision matrix do only apply if the convergence in the regular regions of the mesh is guaranteed [Rei95, Zor97].

In the following we present a general technique for the analysis of subdivision schemes on regular meshes which we will use to prove the smoothness of the $\sqrt{3}$ -subdivision limit surface. Nevertheless, the technique also applies to a larger class of non-standard subdivision schemes. Another analysis technique that is also based on a matrix formulation is used in [War00].

Regular meshes

Instead of using the standard generating function notation for the handling of subdivision schemes [Dyn91], we propose a new matrix formulation which is much easier to handle due to the analogy with the treatment of the irregular case. In fact, rotational symmetries of the subdivision rules are reflected by a blockwise circulant structure of the respective matrices just like in the vicinity of extraordinary vertices. Our matrix based analysis requires only a few matrix computations which can easily be performed with the help of Maple or MatLab. In contrast, the manipulation of the corresponding generating functions would be quite involved if the subdivision scheme does not have a simple factorization (cf. [CDM91, Dyn91]).

To prove the contractivity of some difference scheme, it is sufficient to consider a local portion of a (virtually) infinite regular triangulation. This is due to the shift invariance of the subdivision scheme (*stationary* subdivision). Hence, similarly to the treatment of extraordinary vertices, we can pick an arbitrary vertex \mathbf{p} and a

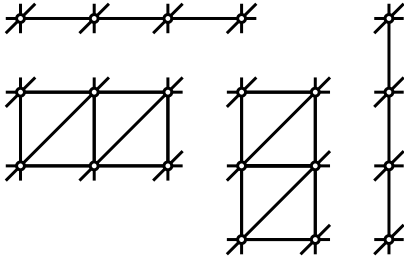


Figure 14: The support of a directional difference includes the vertices that contribute to it. Here we show the supports of D_{10}^3 , $D_{01}D_{10}^2$, $D_{01}^2D_{10}$, and D_{01}^3 .

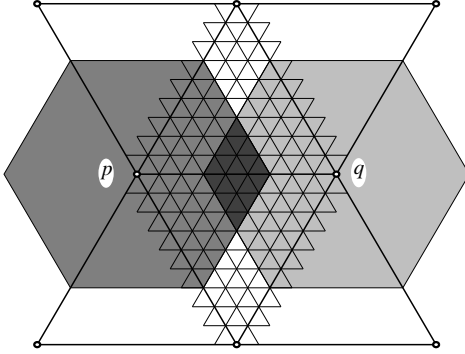


Figure 15: The two refined neighborhoods $S^m(\mathbf{V}_p)$ and $S^m(\mathbf{V}_q)$ (grey areas) of the (formerly) adjacent vertices \mathbf{p} and \mathbf{q} have to overlap (dark area) such that every possible directional difference can be computed from either one.

sufficiently large neighborhood \mathbf{V} around it. The size of this neighborhood is determined by the order n of the differences that we want to consider and by the number m of subdivision steps we want to combine (the analysis of one single subdivision step often does not yield a sufficient estimate to prove contractivity). For a given subdivision scheme S the neighborhoods have to be chosen such that for two adjacent vertices \mathbf{p} and \mathbf{q} in \mathcal{M}_k the corresponding sets $S^m(\mathbf{V}_p)$ and $S^m(\mathbf{V}_q)$ in the refined mesh \mathcal{M}_{k+m} have enough overlap to guarantee that the support of each n th order directional difference is contained in either one (cf. Fig 14).

In our case we want to prove C^2 continuity and hence have to show contractivity of the 3rd directional difference scheme. For technical reasons we always combine an even number of $\sqrt{3}$ -subdivision steps since this removes the 30 degree rotation of the grid directions (just like we did in Section 3). To guarantee the required overlap, we hence have to use a 3-ring neighborhood if we analyse one double $\sqrt{3}$ -step and a 6-ring neighborhood if we analyse two double $\sqrt{3}$ -steps. The corresponding subdivision matrices are 37×37 and 127×127 respectively (cf. Fig 15).

We start by introducing some notation: A regular triangulation is equivalent to the three directional grid which is spanned by the directions

$$\mathbf{v}_{01} = \begin{pmatrix} 1 \\ 0 \end{pmatrix}, \quad \mathbf{v}_{10} = \begin{pmatrix} 0 \\ 1 \end{pmatrix}, \quad \mathbf{v}_{11} = \begin{pmatrix} 1 \\ 1 \end{pmatrix}$$

in index space. Hence the two types of triangular faces in the mesh are given by $\triangle(\mathbf{p}_{i,j}, \mathbf{p}_{i+1,j}, \mathbf{p}_{i+1,j+1})$ and $\triangle(\mathbf{p}_{i,j}, \mathbf{p}_{i+1,j+1}, \mathbf{p}_{i,j+1})$. Accordingly, we define the three directional difference operators

$$D_{uv} : \mathbf{p}_{i,j} \mapsto \mathbf{p}_{i+u,j+v} - \mathbf{p}_{i,j}$$

with $(u, v) \in \{(1, 0), (0, 1), (1, 1)\}$. If we apply these difference operators D_{uv} to a finite neighborhood \mathbf{V} we obtain all possible differ-

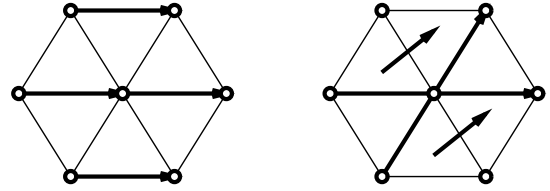


Figure 16: Directional differences on a finite neighborhood \mathbf{V} . Left: the application of D_{10} yields four different vectors. Right: the application of J_2 yields four vectors, one for D_{10}^2 , one for D_{01}^2 and two "twist" vectors for the mixed derivative $D_{10}D_{01}$.

ences where both $\mathbf{p}_{i,j}$ and $\mathbf{p}_{i+u,j+v}$ are elements of \mathbf{V} . For a fixed neighborhood \mathbf{V} the operator D_{uv} can be represented by a matrix that has two non-zero entries in every row, e.g.,

$$\mathbf{V} = \left\{ \begin{pmatrix} 0 \\ 0 \end{pmatrix}, \begin{pmatrix} 1 \\ 0 \end{pmatrix}, \begin{pmatrix} 1 \\ 1 \end{pmatrix}, \begin{pmatrix} 0 \\ 1 \end{pmatrix}, \begin{pmatrix} -1 \\ 0 \end{pmatrix}, \begin{pmatrix} -1 \\ -1 \end{pmatrix}, \begin{pmatrix} 0 \\ -1 \end{pmatrix} \right\}$$

implies

$$D_{10} = \begin{pmatrix} -1 & 1 & 0 & 0 & 0 & 0 & 0 \\ 0 & 0 & 1 & -1 & 0 & 0 & 0 \\ 1 & 0 & 0 & 0 & -1 & 0 & 0 \\ 0 & 0 & 0 & 0 & 0 & -1 & 1 \end{pmatrix}.$$

See Fig. 16 for a geometric interpretation. Based on the difference operators, we can build the *Jet-operators*

$$J_1 = \begin{pmatrix} D_{10} \\ D_{01} \end{pmatrix} \quad J_2 = \begin{pmatrix} D_{10}D_{10} \\ D_{10}D_{01} \\ D_{01}D_{01} \end{pmatrix} \quad J_3 = \begin{pmatrix} D_{10}D_{10}D_{10} \\ D_{10}D_{10}D_{01} \\ D_{10}D_{01}D_{01} \\ D_{01}D_{01}D_{01} \end{pmatrix} \quad (10)$$

which map the control vertices in \mathbf{V} to the complete set of independent directional differences $J_n(\mathbf{V})$ of a given order n .

Let S be the subdivision scheme which maps control vertices $\mathbf{p}^{(k)}$ from the k th refinement level to the $(k+1)$ st refinement level $\mathbf{p}^{(k+1)} = S(\mathbf{p}^{(k)})$. Again, if we consider the action of S on a local neighborhood \mathbf{V} only, we can represent S by a matrix with each row containing an affine combination that defines the position of one new control vertex.

For the convergence analysis we need a so-called *difference scheme* S_n which maps the differences $J_n(\mathbf{V}^{(k)})$ directly to $J_n(\mathbf{V}^{(k+1)}) = J_n(S(\mathbf{V}^{(k)})) = S_n(J_n(\mathbf{V}^{(k)}))$. From [Dyn91] it is well-known that the subdivision scheme S generates C^n limit surfaces (for regular control meshes) if the scheme $h^n S_{n+1}$ is contractive, i.e., if $\|S_{n+1}\| \leq q < h^{-n}$ with respect to an appropriate matrix norm. Here, the factor h^n takes the implicit parameterization into account. For subdivision schemes which are based on the dyadic split operation, edges are bi-sected in every step and hence $h = 2$. This is true for all standard schemes. However, for our new $\sqrt{3}$ -subdivision scheme we have to choose $h = 3$ since we are analysing the double application of the $\sqrt{3}$ -operator which corresponds to an edge tri-section.

In the univariate case these difference schemes S_n can be obtained by simple factorization of the corresponding generating function representations. In the bivariate case the situation is much more difficult since *jets* are mapped to *jets*! In general we cannot find a simple scheme which maps, e.g., the differences $D_{10}(\mathbf{V})$ to $D_{10}(S(\mathbf{V}))$ because the directional differences are not independent from each other. Hence we have to find a more general matrix scheme

$$\begin{pmatrix} D_{10}(S(\mathbf{V})) \\ D_{01}(S(\mathbf{V})) \end{pmatrix} = S_1 \begin{pmatrix} D_{10}(\mathbf{V}) \\ D_{01}(\mathbf{V}) \end{pmatrix}$$

which maps $J_1(\mathbf{V})$ to $J_1(S(\mathbf{V}))$ by allowing $D_{10}(S(\mathbf{V}))$ to depend on both $D_{10}(\mathbf{V})$ and $D_{01}(\mathbf{V})$. As this construction requires quite

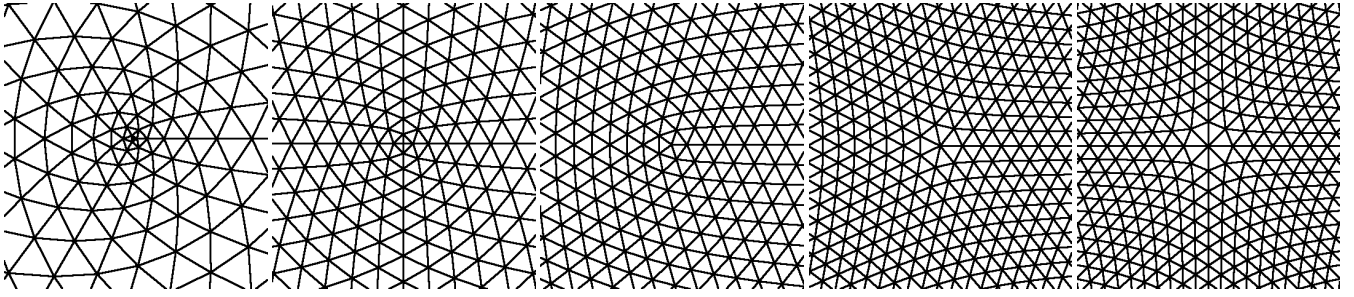


Figure 17: The local regularity of the subdivision surface at extraordinary vertices requires the injectivity of the characteristic map. We show the isoparameter lines for these maps in the vicinity of irregular vertices with valence $n = 3, 4, 5, 7$, and 8 (from left to right).

involved factorizations and other polynomial transformations, we now suggest a simpler approach where most of the computation can be done automatically.

Let J_n be the n th jet-operator restricted to \mathbf{V} and J_n^{-1} its SVD pseudo-inverse. Because J_n has a non-trivial kernel (containing all configurations where the points in \mathbf{V} are uniformly sampled from a degree $n - 1$ polynomial) its inverse cannot be well-defined. At least we know that

$$J_n J_n^{-1} J_n = J_n$$

which means that if J_n^{-1} is applied to a set of n th order differences $J_n(\mathbf{V})$ it reconstructs the original data up to an error \mathbf{e} which lies in the kernel of J_n , i.e., $J_n^{-1}(J_n(\mathbf{V})) = \mathbf{V} + \mathbf{e}$ with $J_n(\mathbf{e}) = \mathbf{0}$.

If the subdivision scheme S has polynomial precision of order $n - 1$ this implies that S maps the kernel of J_n into itself:

$$S(\ker(J_n)) \subset \ker(J_n). \quad (11)$$

As a consequence $J_n(S(\mathbf{e})) = \mathbf{0}$ as well, and therefore

$$J_n S J_n^{-1} J_n = J_n S.$$

Since the operator on the right hand side of this equation maps the vertices of the control mesh $\mathbf{V}^{(k)}$ to the n th differences on the next refinement level $J_n(\mathbf{V}^{(k+1)})$, the operator

$$S_n := J_n S J_n^{-1} \quad (12)$$

does map the n th differences $J_n(\mathbf{V}^{(k)})$ directly to the n th differences on the next level $J_n(\mathbf{V}^{(k+1)})$. This is exactly the difference scheme that we have been looking for! In order to prove the convergence of the subdivision scheme, we have to show that the maximum norm of $h^{n-1}S_n$ is below 1. Alternatively, it is sufficient to show that the maximum singular value of the matrix $h^{n-1}S_n$ is smaller than 1 since this provides a monotonically decreasing upper bound for the maximum n th difference.

To verify the polynomial precision (11) for a given subdivision matrix S we first generate another matrix K whose columns span the kernel of J_n . Notice that the dimension of $\ker(J_n)$ is the dimension of the space of bivariate degree $n - 1$ polynomials which is $\dim \Pi_{n-1}^2 = \frac{1}{2}(n+1)n$. The matrix K can be read off from the SVD decomposition of J_n [GvL96]. The polynomial reproduction is then guaranteed if the equation

$$SK = XK \quad (13)$$

has a matrix solution $X = (K^T K)^{-1} K^T S K$. If this is satisfied, we find the n th difference scheme S_n by (12).

For the analysis of our $\sqrt{3}$ -subdivision scheme we let \mathbf{V} be the 6-ring neighborhood of a vertex which consists of 127 vertices. Let S be the single-step $\sqrt{3}$ -subdivision matrix, R be the back-rotation-by-permutation matrix and D_{10} the directional difference matrix. Although these matrices are quite large, they are very sparse and

can be constructed quite easily (by a few lines of MatLab-code) due to their block-circulant structure.

From these matrices we compute $\tilde{S} = RS^2$ and a second directional difference operator $D_{01} = R^2 D_{10} R^{-2}$. The two directional differences are combined to build the 3rd order jet-operator J_3 (cf. (10)). Here we use the 3rd differences since we want to prove C^2 continuity. From the singular value decomposition of J_3 we obtain the matrix K whose columns span the kernel of J_3 and the pseudo-inverse J_3^{-1} . The matrix K is then used to prove the quadratic precision of S (cf. (13)) and the pseudo-inverse yields the difference scheme $\tilde{S}_3 = J_3 \tilde{S} J_3^{-1}$. The contractivity of the 3rd order difference scheme finally follows from the numerical estimation $\|\tilde{S}_3\| = \|J_3 \tilde{S} J_3^{-1}\| \leq 0.78 \times 3^{-4}$ which proves that the $\sqrt{3}$ -subdivision scheme S generates C^2 surfaces for regular control meshes.

Extraordinary vertices

In the vicinity of the extraordinary vertices with valence $\neq 6$ we have to apply a different analysis technique. After the convergence in the regular mesh regions (which for subdivision meshes means "almost everywhere") has been shown, it is sufficient to analyse the behavior of the limit surface at the remaining isolated extraordinary points.

The intuition behind the sufficient convergence criteria by [Rei95, Zor97, Pra98] is that the representation of the local neighborhood \mathbf{V} with respect to the eigenvector basis of the local subdivision matrix S corresponds to a type of Taylor-expansion of the limit surface at that extraordinary point. Hence, the eigenvectors ("eigenfunctions") have to satisfy some regularity criteria and the leading eigenvalues have to guarantee an appropriate scaling of the tangential and higher order components of the expansion. Especially the conditions (5) have to be satisfied for all valences $n = 3, \dots, n_{\max}$.

When checking the eigenstructure of the subdivision matrix S we have to use a sufficiently large r -ring neighborhood \mathbf{V} of the center vertex \mathbf{p} . In fact the neighborhood has to be large enough such that the regular part of it defines a complete surface ring around \mathbf{p} by itself [Rei95]. In the case of $\sqrt{3}$ -subdivision we hence have to use $r = 4$ rings around \mathbf{p} (since 4 is the diameter of the subdivision basis function's support). This means we have to analyse a $(10n+1) \times (10n+1)$ matrix where n is \mathbf{p} 's valence.

Luckily the subdivision matrix S has a block circulant structure and it turns out that the leading eigenvalues of S are exactly the eigenvalues we found in (4). Since those eigenvalues satisfy (5) we conclude that the matrix S has the appropriate structure for C^1 convergence.

The exact condition on the eigenvectors and the injectivity of the corresponding characteristic map are quite difficult to check strictly. We therefore restrict ourselves to the numerical verification by sketching the iso-parameter lines of the characteristic map in Fig. 17.